

Finite element analysis of sustainable flexible pavements reinforced with coir geotextiles

Chetan Bhole, Anusudha V., V. Sunitha and Samson Mathew

Department of Civil Engineering, National Institute of Technology, Tiruchirappalli, India crbhole@ci.vjti.ac.in

Available online at: www.isca.in, www.isca.me

Received 15th July 2025, revised 25th August 2025, accepted 9th September 2025

Abstract

Reinforcement of flexible pavements using geosynthetics is a proven technique for enhancing structural performance, increasing service life, and reducing maintenance costs. This study focuses on the utilization of woven coir geotextiles as a sustainable reinforcement material for flexible pavements constructed over high-plasticity organic subgrade soils. A set of small-scale in-box plate load experiments was performed to evaluate the response of reinforced and unreinforced pavement sections under static circular loading, using a 150 mm diameter mild steel plate. Testing encompassed both uniform subgrade conditions and layered setups, where H2M5 and H2M6 coir geotextiles were placed between the subgrade and subbase layers. These experiments aimed to evaluate the structural contribution of coir reinforcement in improving pavement response. In addition to physical testing, a detailed finite element analysis (FEA) using ABAQUS software was carried out to simulate pavement behavior and gain further insights into displacement, stress, and strain patterns under loading. The results from both laboratory and numerical studies revealed significant improvements in performance with coir geotextile reinforcement. The H2M5-reinforced section exhibited a 29% reduction in surface displacement and a 21% decrease in vertical strain on the subgrade compared to the unreinforced section. Reduced deformation and strain were also observed at radial distances up to 1 meter from the load center, indicating improved load distribution characteristics. These findings demonstrate that coir geotextiles, particularly H2M5, can substantially enhance the structural behavior of flexible pavements over weak subgrades, offering a sustainable and eco-friendly alternative for reinforcing low-volume roads.

Keywords: Subgrade, Coir geotextiles; Static plate load test; FEA; Surface displacement; Vertical strain.

Introduction

In India, rural roads form a vital component of the transportation network by connecting villages to towns and urban centers, thereby enabling mobility, trade, and access to essential services. Traditionally, roads carrying less than 450 commercial vehicles per day (CVPD) have been considered low-volume roads as per IRC: SP:72-2007, although the latest IRC: SP:72 design framework uses cumulative traffic in terms of equivalent standard axles (ESALs). Nevertheless, this threshold remains a useful indicator of the traffic magnitude typical of village roads. The construction and maintenance of these roads are often complicated by the presence of weak or organic subgrade soils that exhibit unfavourable geotechnical properties, including high compressibility, poor load-bearing capacity, and significant water sensitivity. These characteristics accelerate pavement distress through differential settlements, moisture-induced degradation, and premature failures. Since organic or weak soils are widespread, avoiding them is often impractical. Instead, in-situ stabilization or structural mitigation techniques are essential for ensuring cost-effective and durable road construction¹. Conventional improvement techniques, such as chemical stabilization with lime or cement and mechanical compaction, have long been used to prepare a stable platform for pavement layers. However, over the past few decades,

geosynthetics have gained substantial attention as an alternative solution for subgrade improvement, particularly for low-volume roads where cost and construction constraints are critical. Geosynthetics, first introduced in roadway applications in the 1960s², offer multiple functions including reinforcement, separation, filtration, and improved drainage. Literature indicates that their benefits are especially pronounced in pavements constructed over weak subgrades and thin base layers, where reinforcement can significantly extend service life or allow for reductions in layer thickness³.

In flexible pavement design, one of the primary challenges is the development of horizontal stresses at the interfaces of pavement layers under traffic loading, which can lead to localized deformations and rutting. Incorporating a geosynthetic layer acts both as a separator and as reinforcement, modifying the stress distribution and allowing traffic loads to spread over a broader area. This improved load dispersion reduces strain accumulation and offers two primary design benefits: the pavement can sustain greater traffic without increasing thickness, or the overall pavement thickness can be reduced while maintaining equivalent structural performance⁴. The efficiency of this reinforcement mechanism depends on various factors such as subgrade strength, the mechanical and hydraulic properties of the geosynthetic, base thickness, and the placement

position of the reinforcement⁵⁻⁸. Studies have consistently shown that the improvement achieved through geosynthetic reinforcement is more significant for pavements over weak subgrades compared to those with moderate or high bearing capacities⁹. Among the different geosynthetic materials, natural fiber geotextiles, particularly coir-based products have gained attention due to their environmental and economic advantages. Coir geotextiles are biodegradable, locally available, and cost-effective. Their rough surface texture provides excellent interfacial friction with surrounding soils, which can enhance reinforcement performance compared to certain synthetic materials¹⁰.

Furthermore, the tensioned membrane effect, which is a key mechanism of reinforcement, becomes active when vertical deflection occurs. Rural roads, which allow greater permissible rut depths, facilitate the full mobilization of this effect, enabling coir geotextiles to significantly improve the load-bearing capacity and service life of such pavements¹¹.

Determining the optimum placement of a geosynthetic layer within the pavement structure has been a persistent research focus, as its position significantly affects performance. While different studies report varying conclusions, many have emphasized that placing reinforcement at the subgrade—subbase interface is particularly effective in controlling rutting, reducing subbase thickness, and maintaining the structural integrity of pavement layers by preventing contamination from fine particles migrating upward from the subgrade 12. The reinforcement primarily functions by mobilizing tensile forces under traffic loading and by developing interfacial shear resistance with the surrounding soil 13.

Building upon experimental findings, finite element (FE) analysis has emerged as a powerful tool for evaluating the internal behavior of reinforced pavements, including strain distribution, stress transfer, and permanent deformations. By simulating realistic traffic and environmental conditions, FE modeling complements laboratory tests and helps in the optimization of reinforcement materials and placement strategies. The use of ABAQUS for modeling geogridreinforced pavements has shown promising results, with studies reporting up to a 20% reduction in rut depth under a single load cycle due to reinforcement¹⁴. Response models incorporating membrane elements to represent the geosynthetic layer have successfully linked vertical strain and bulk stress parameters with long-term performance indicators¹⁵. Finite element analysis of geosynthetic placement within the base layer has demonstrated reductions in both vertical and shear strains at the top of the subgrade¹⁶.

In the context of low-volume roads, geogrid reinforcement has been associated with an 18% decrease in vertical strain at the subgrade surface and a 68% reduction in tensile strain at the bottom of the asphalt layer¹⁷. Reinforced pavement sections over weak subgrades have also exhibited significant reductions

in surface deformation, along with a traffic benefit ratio of approximately 3.7¹⁸.

To validate numerical findings and quantify real-world performance, laboratory studies remain essential. Plate load tests are commonly conducted to evaluate the load-bearing and settlement characteristics of reinforced and unreinforced sections. For effective reinforcement, the geosynthetic layer is typically placed at the subbase—subgrade interface, where it can best contribute to reducing rutting and improving overall pavement performance.

Coir geotextiles are manufactured in standardized grades (H2M1–H2M10), with nominal mesh sizes ranging from approximately 3 mm to 25 mm (1/8 in. to 1 in.). Indian Standard IS 15869:2008 classifies these products into weight-based grades—Grade I (~400 g/m²), Grade II (~700 g/m²), and Grade III (~900 g/m²)—for various civil engineering applications, including road reinforcement. In this study, woven coir products of Grade I (H2M6) and Grade II (H2M5) were selected and installed at the subbase–subgrade interface to evaluate their structural contribution in low-volume pavement sections ¹⁹.

The investigation combines experimental and numerical approaches: laboratory plate load tests are conducted to determine the elastic modulus of both reinforced and unreinforced sections, while finite element modeling in ABAQUS is employed to evaluate stresses, strains, and displacements. This combined methodology enables a comprehensive assessment of the structural benefits of coir geotextile reinforcement and identifies opportunities for optimizing material usage and reducing construction costs.

Characterization of Materials

This section outlines the engineering properties and specifications of the subgrade soil, granular sub-base material, and coir geotextiles used in the study.

Subgrade Soil Properties: The subgrade soil employed in this investigation is an organic soil characterized by high plasticity. Its physical and engineering properties, determined through a series of laboratory tests in accordance with relevant Indian Standards, are summarized in Table-1.

A specific gravity of 2.2 confirms the presence of organic content, indicating its poor suitability as a natural subgrade material. Based on the soil classification system of IS 1498:1970, the soil is categorized as OH (high plastic organic soil). The Standard Proctor Compaction Test (IS 2720, Part VIII) was carried out to determine the Maximum Dry Density (MDD) and Optimum Moisture Content (OMC). The sample compacted at OMC was subjected to a California Bearing Ratio (CBR) test (IS 2720, Part XVI), which resulted in a low CBR value of 3.7%, indicating the need for reinforcement²⁰.

Table-1: Mechanical and physical properties of the tested soil.

Engineering property	Value
Liquid limit (%)	53
Plasticity index (%)	23
IS classification	ОН
Specific gravity	2.200
Optimum Moisture Content (%)	26
Maximum Dry Density (g/cc)	1.58
California Bearing Ratio (%)	3.7

Granular Sub-base (GSB) Characteristics: The sub-base layer consists of crushed stone material conforming to Grading III of GSB specifications as per MORD Clause 401.2.1. The engineering properties, listed in Table-2, were verified against ASTM D 1241-15 limits. Since variations in material gradation or strength can significantly affect the elastic modulus and pavement performance, strict quality control measures were implemented to ensure consistency in the source of GSB material throughout the study.

Table-2: Engineering properties of the GSB material.

Engineering property	Value	
Specific gravity	2.730	
Aggregate Impact value (%)	24	
Optimum Moisture Content (%)	6	
Maximum Dry Density (g/cc)	2.21	
California Bearing Ratio (%)	30	

Coir Geotextile Reinforcement: Two types of coir geotextiles, H2M5 (Grade II) and H2M6 (Grade I), were incorporated as reinforcement layers to enhance the structural behavior of the test sections. Their specifications, obtained from IS 15868 (Parts 1–6) and IS 13162 (Part 5)²¹, are detailed in Table-3. The physical appearance and weave structures of the coir geotextiles are illustrated in Figure-1.

Laboratory Plate Load Testing

The laboratory plate load testing aimed to evaluate the bearing response and load–settlement characteristics of model pavement sections incorporating a coir geotextile interlayer, with a particular focus on determining potential reductions in granular sub-base (GSB) thickness while maintaining performance.

Model pavement sections were prepared in a rigid welded mildsteel tank of internal dimensions 1.20 m x 1.20 m x 0.75 m. The subgrade consisted of pulverised organic soil, compacted in 50 mm thick layers to achieve a total thickness of 450 mm. For each lift, the required soil quantity was calculated based on the maximum dry density (MDD) and adjusted to the optimum moisture content (OMC) prior to mixing and compaction. Uniformity in compaction was verified by sampling at multiple locations using a thin-walled cylindrical tubesfor in situ moisture content and density measurement. A compacted GSB layer was then placed over the subgrade, with or without an intervening coir geotextile layer, to create different test configurations. The test matrix included: (i) an unreinforced control section with full GSB thickness (~175 mm), (ii) a reduced-thickness GSB section (125 mm), and (iii) sections with 125 mm GSB reinforced using coir geotextiles H2M5 and H2M6. These configurations are outlined in Table 4 and illustrated in Figure-2.

Table-3: Specifications of Coir Geotextile ¹⁹⁻²¹.

Parameters	H2M5	H2M6
Aperture size (mm * mm)	9*9	20*20
Thickness (mm)	9	7
Threads per dm (nos.)	11*7	4.5*4.5
Width (mm)	1500	1500
Weight (g/sqm)	740	400
Tensile strength warp *weft (kN/m)	20*18	18*15
Water holding capacity on dry weight (%)	500	500
Puncture resistance (N)	500	440



Figure-1a: H2M5 coir geotextile.

Vol. 14(3), 23-33, September (2025)



Figure-1b: H2M6 coir geotextile. **Figure-1:** Types of coir geotextiles used.

Table 4: Details of the test section configurations.

Section	Thickness (m)				
	Subgrade	Coir mat (H2M5)	Coir mat (H2M6)	GSB	
Section 1	0.45	-	-	-	
Section 2	0.45	-	-	0.175	
Section 3	0.45	-	-	0.125	
Section 4	0.45	0.009	-	0.125	
Section 5	0.45	-	0.007	0.125	

The loading setup, shown in Figure-3, comprised a rigid selfreacting steel frame and a centrally mounted hydraulic jack with a 30-tonne capacity (≈300 kN). A 50 kN proving ring was employed for precise load measurements. Load was applied through a circular mild-steel plate of 150 mm diameter and 25 mm thickness. Settlements were recorded using two dial gauges placed diametrically opposite each other and mounted on independent reference beams. The average of the two readings was taken as the settlement. The tank dimensions were selected to maintain a width-to-plate diameter ratio > 5, minimizing boundary effects. An initial seating pressure of 0.07 kg/cm² (~7 kPa) was applied to ensure proper contact between the plate and the surface. Subsequent loading was performed in increments designed to produce approximately 0.25 mm settlement. Each load step was maintained until the rate of settlement reduced to below 0.025 mm/min. Testing continued until the cumulative settlement approached 1.75 mm. Load and deformation data were recorded manually from the proving ring and dial gauges. The test data were used to back-calculate the subgrade elastic modulus (Es). The contact pressure for each increment was calculated and the stabilized settlement was determined as the average of the gauge readings minus the initial seating settlement. The modulus of subgrade was estimated using the expression

$$E_{subgrade} = \frac{\pi \sigma a}{2 \Delta} (1 - \mu^2) \tag{1}$$

where $E_{subgrade}$ = Elastic modulus of subgrade; σ = applied stress; a = radius of plate; Δ = deflection of plate at applied stress σ and μ = Poisson's ratio.

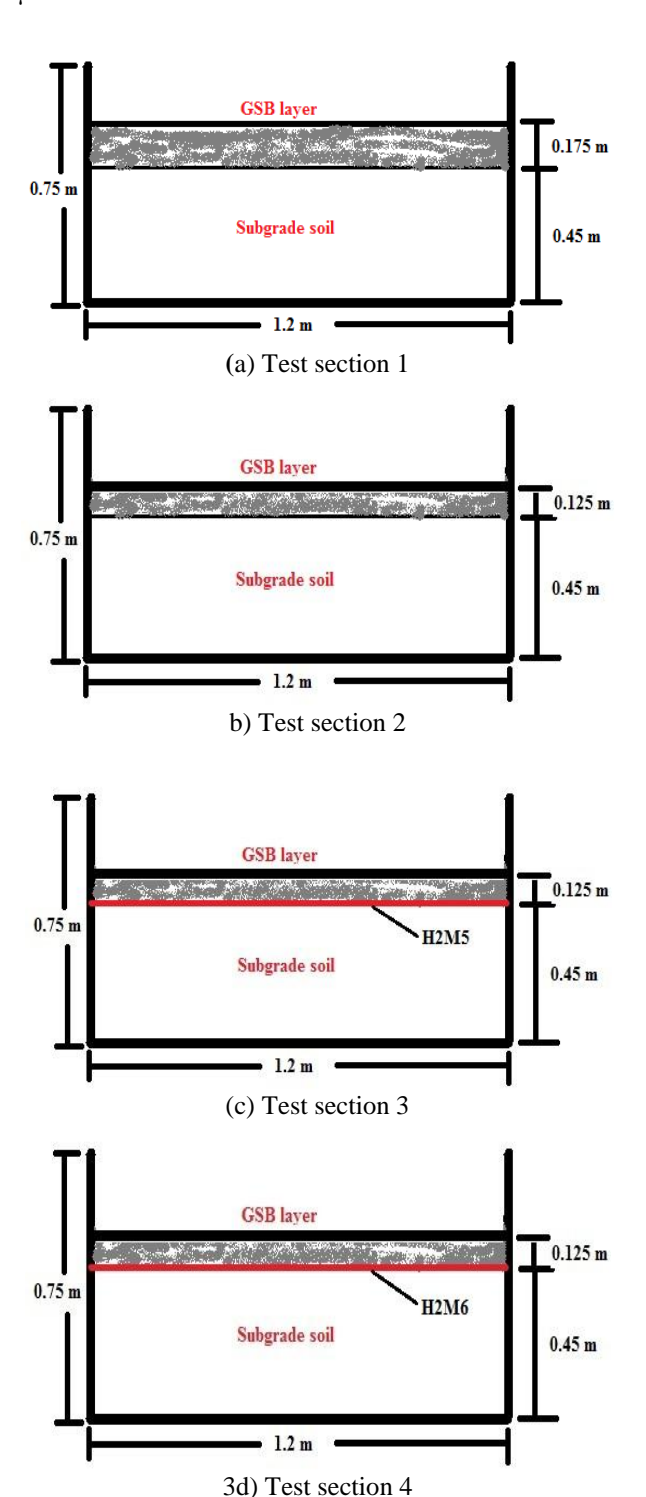


Figure-2: Test sections used for plate load test.

For layered configurations, the elastic modulus of the GSB layer was computed using Burmister's two-layer theory. The subgrade modulus obtained above was kept constant, and the GSB modulus was iteratively determined to match observed settlements. Burmister's formulation for surface deflection under a rigid circular plate is expressed as:

$$\Delta = \frac{1.18 \,\mathrm{pa}}{\mathrm{E}_{\mathrm{subgrade}}} \,\mathrm{F}_{2} \tag{2}$$

Where: Δ = surface deflection, $E_{subgrade}$ = Modulus of Elasticity of subgrade, p = Unit load on the circular plate, a = Radius of plate, F_2 = Two layer deflection factor.



Figure-3a: Plate load test setup on subgrade.



Figure-3b: Tank setup with geotextile layer. **Figure-3**: Plate load test setup.

Results and Discussion

The modulus of subgrade reaction (K) for each test section was determined by extracting pressure values corresponding to a settlement of 0.125 cm from the load–settlement curves shown in Figure-4 and applying the theoretical equations described previously. The comparison of Sections 2 and 3 reveals that the increase in GSB thickness from 125 mm to 175 mm

significantly improves load dispersion, resulting in higher bearing capacity and reduced settlement.

Section 2 (175 mm GSB, unreinforced) recorded a bearing capacity of 300 kPa at 5 mm settlement, whereas Section 3 (125 mm GSB, unreinforced) reached only 260 kPa, underlining the importance of GSB thickness in resisting deformation. When coir geotextiles were incorporated, marked improvements were observed. Section 4 (H2M5 reinforcement with 125 mm GSB) showed a peak bearing capacity of 306 kPa, and Section 5 (H2M6 reinforcement with 125 mm GSB) achieved 282 kPa. In contrast, the control subgrade section (Section 1) registered only 143 kPa.

These findings underscore the ability of coir geotextiles to substitute for lost GSB thickness by enhancing stiffness and load distribution. The 18% improvement in bearing capacity in Section 4 relative to Section 3 demonstrates the superior reinforcing effect of the H2M5 geotextile. Section 5 also exhibited improvement (8%), though to a lesser degree, likely due to its larger aperture size and lower confinement capability. In Section 5, the load-settlement response initially paralleled that of the unreinforced Section 3, indicating delayed mobilization of tensile resistance. However, as settlements progressed beyond 3.5 mm, lateral confinement improved and the reinforcement began to contribute more effectively. This delayed engagement suggests that geotextiles with finer apertures like H2M5 provide earlier and more efficient reinforcement.

The elastic moduli derived from Burmister's method, summarized in Table 5corroborate these trends. Reinforced sections showed higher stiffness values, with Section 4 having the highest Es among all configurations. The geotextile layer, acting as a tensile membrane, resists differential settlements by mobilizing tension at the interface between the GSB and subgrade. This mechanism enhances stress distribution and reduces local deformations, requiring higher applied pressures to reach equivalent settlements.

Overall, the inclusion of H2M5 coir geotextile demonstrates significant technical benefit by improving pavement response under load, enabling GSB reduction without compromising performance. The findings advocate for the use of coir geotextiles in low-volume flexible pavements, balancing mechanical function with economic feasibility.

Finite element analysis of reinforced pavement sections using abaqus: To simulate the mechanical behavior of reinforced and unreinforced flexible pavement systems, a finite element modeling approach was employed using ABAQUS. The pavement was conceptualized as a layered system resting on a deformable subgrade, with static surface loading applied to represent traffic-induced stresses. The study investigated several pavement configurations with varying GSB thicknesses and the presence or absence of coir geotextile reinforcement, as detailed in Table-6.

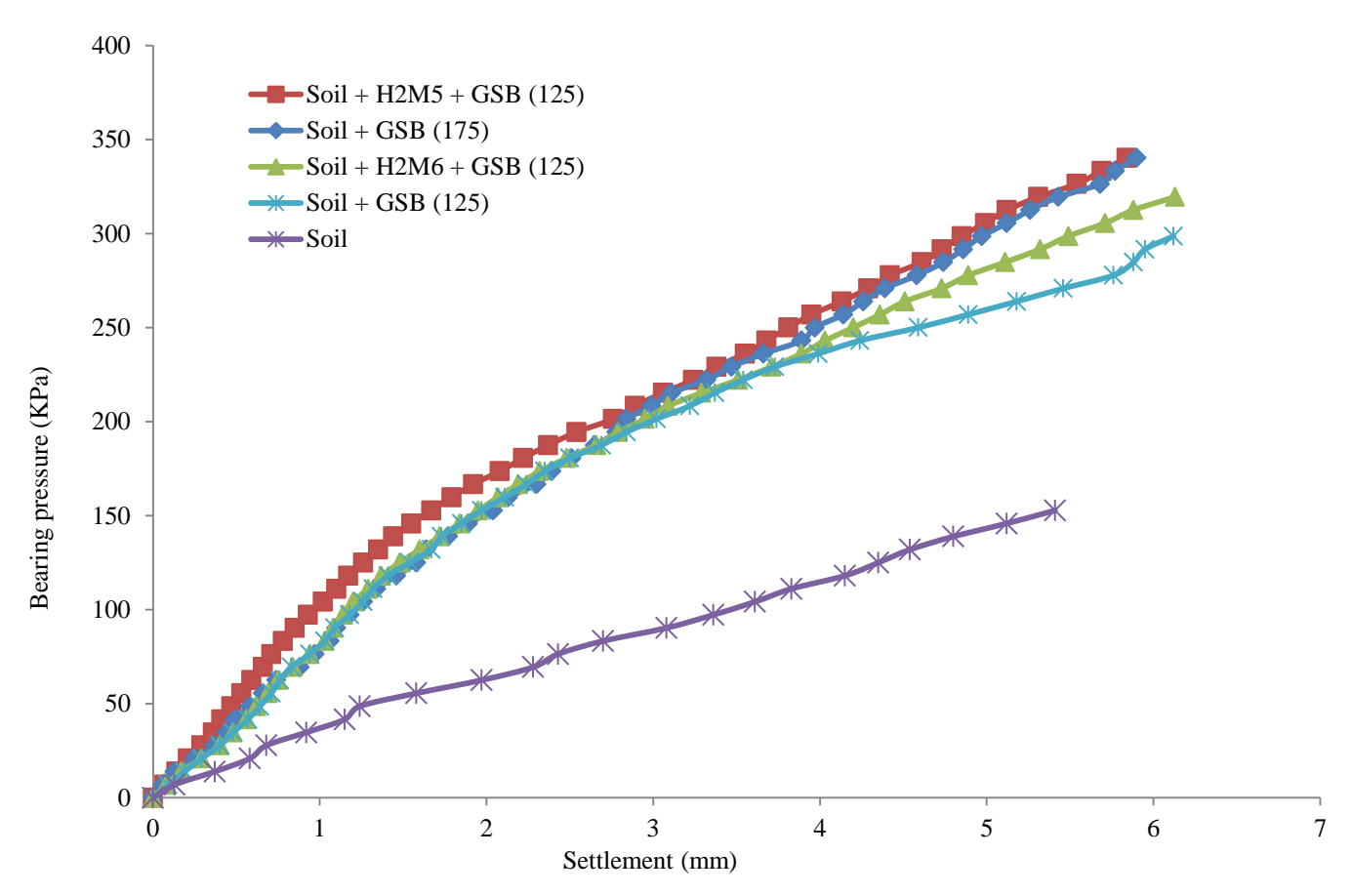


Figure-4: Bearing capacity versus settlement curve for the test sections.

Table-5: Layer modulus computed from pressure – deflection curves

Section	Subbase layer thickness (mm)	Deflection factor (F ₂)	h/a ratio	Ratio of modulus	Effective Elastic Modulus (kPa)
Soil	-	-	-	-	5917
Soil+GSB (175 mm)	175	0.56	1.17	7.5	44380
Soil+GSB (125 mm)	175	0.64	0.833	6.0	35501
Soil + GSB (125 mm) + H2M5 layer	125	0.55	0.833	11.0	65091
Soil + GSB (125 mm) + H2M6 layer	125	0.59	0.833	9.0	53266

Table-6: Pavement scenarios and geometries

Pavement scenario	Thickness of asphalt concrete (mm)	Thickness of base course (mm)	Thickness of sub- base course (mm)	Geotextile layer	Thickness of subgrade (mm)
Pavement 1	25	150	175	NA	500
Pavement 2	25	150	125	NA	500
Pavement 2a	25	150	125	H2M5	500
Pavement 2b	25	150	125	H2M6	500

Each pavement section was modelled using a two-dimensional axisymmetric framework, which efficiently captures stress and deformation patterns under circular loading conditions. A 15-node quadratic structural solid element was selected to discretize the geometry, with mesh refinement concentrated in the loading zone to enhance accuracy.

The surface layer was assigned viscoelastic properties to simulate bituminous behavior under sustained loading, while the underlying base, sub-base, and subgrade layers were modeled as linear elastic materials. An input pressure of 560 kPa, corresponding to one-half of a standard axle load (40 kN), was applied over a 150 mm diameter circular contact area. Appropriate boundary conditions were applied, wherein the

model base was constrained in both vertical and horizontal directions, and lateral boundaries were restricted against horizontal movement. The schematic representation of the applied boundary conditions is presented in Figure-5.

Material properties for each layer were derived from experimental results and relevant literature, with particular attention to modulus values obtained through plate load testing, as shown in Table-7. A four-layer configuration was adopted for all pavement sections, maintaining constant thicknesses for the surface and base layers (25 mm and 125 mm, respectively), while the GSB thickness varied across configurations. The subgrade was modelled with a uniform depth of 500 mm.

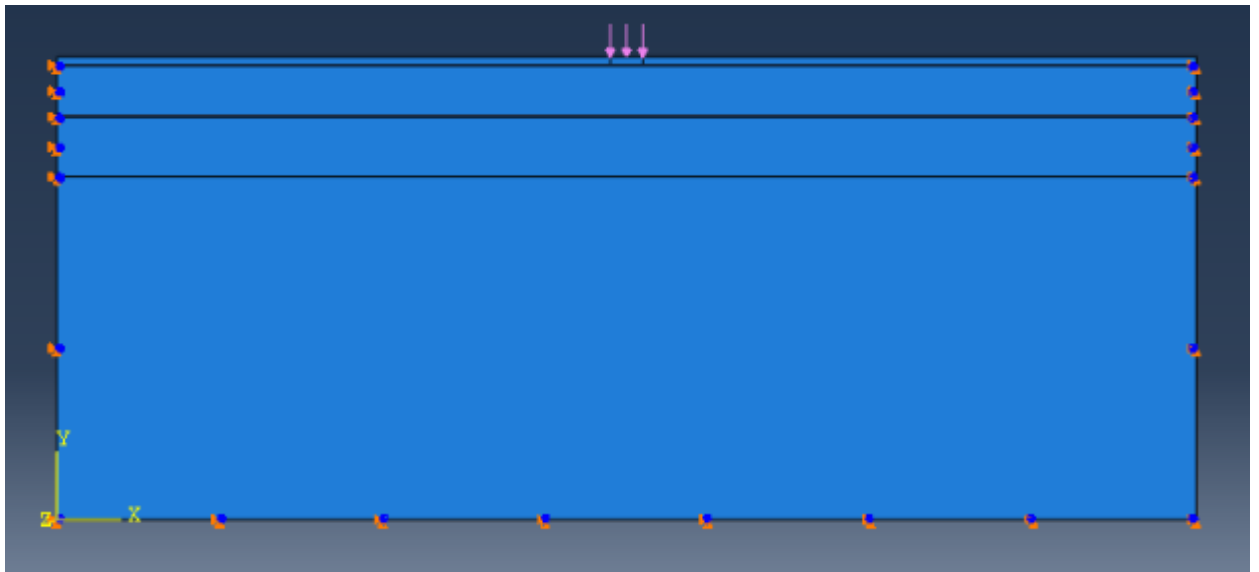


Figure-5: Finite element model for the test section.

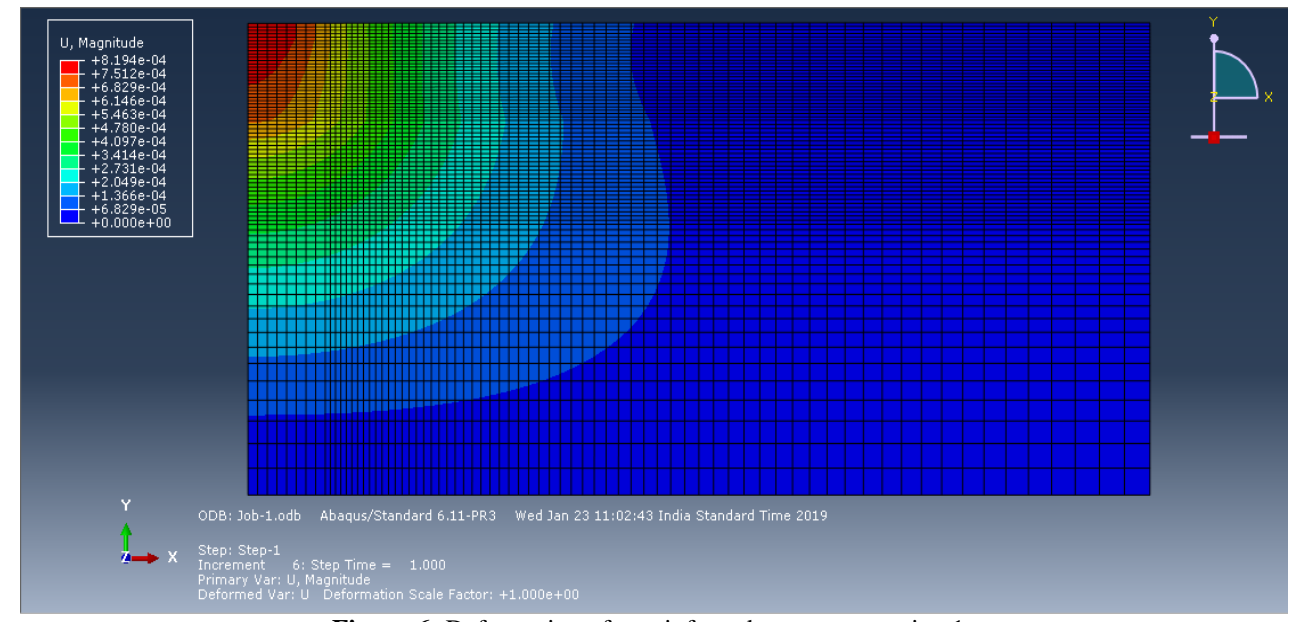


Figure-6: Deformation of unreinforced pavement section 1.

Simulation results revealed distinct differences in surface deformation among the various pavement configurations. For the unreinforced section with a reduced GSB thickness of 125 mm (UR–125), the maximum vertical deflection beneath the applied load was found to be 0.89 mm. In contrast, the configurations reinforced with H2M5 and H2M6 coir geotextiles exhibited reduced settlements of 0.65 mm and 0.73 mm, respectively, as illustrated in Figure 7. This corresponds to a reduction in vertical displacement of approximately 27% for H2M5 and 18% for H2M6, clearly highlighting the stiffness-enhancing effect of geotextile reinforcement.

The observed reduction in settlement for the reinforced pavement sections is attributed to the lateral restraint provided by the geotextile layer at the subgrade–GSB interface. Under loading, shear deformation initiates lateral movement in the

base layer, which is countered by the geotextile through tensile resistance and frictional interlock. This mechanism limits lateral spread and enhances the structural integrity of the composite system, thereby reducing surface deflection.

Further insights into the reinforcement performance were obtained through analysis of subgrade strain response. The maximum compressive vertical strain for the UR–175 mm section was measured at 1256×10^{-6} . This value increased to 1663×10^{-6} for the reduced GSB section, but decreased to 1183×10^{-6} and 1328×10^{-6} for the H2M5- and H2M6-reinforced sections, respectively. These results, presented in Figure 8, indicate a reduction in strain by approximately 29% for H2M5 and 20% for H2M6, affirming the role of coir geotextiles in distributing load and limiting subgrade deformation, even with thinner base layers.

Table-7: Properties of materials adopted for FEM analysis of the pavement scenarios

Material	Surface layer	Base layer	Sub-base layer	Subgrade layer	
Model	Visco elastic	Linear elastic	Linear elastic	Linear elastic	
Thickness (mm)	25	150	125/175	500	
Young's modulus (MPa)	3000	450	Effective Elastic Modulus listed in Table 5		
Poisson's ratio	0.35	0.35	0.35	0.35	
Dry density (kN/m³)	20	19	18.5	17.4	

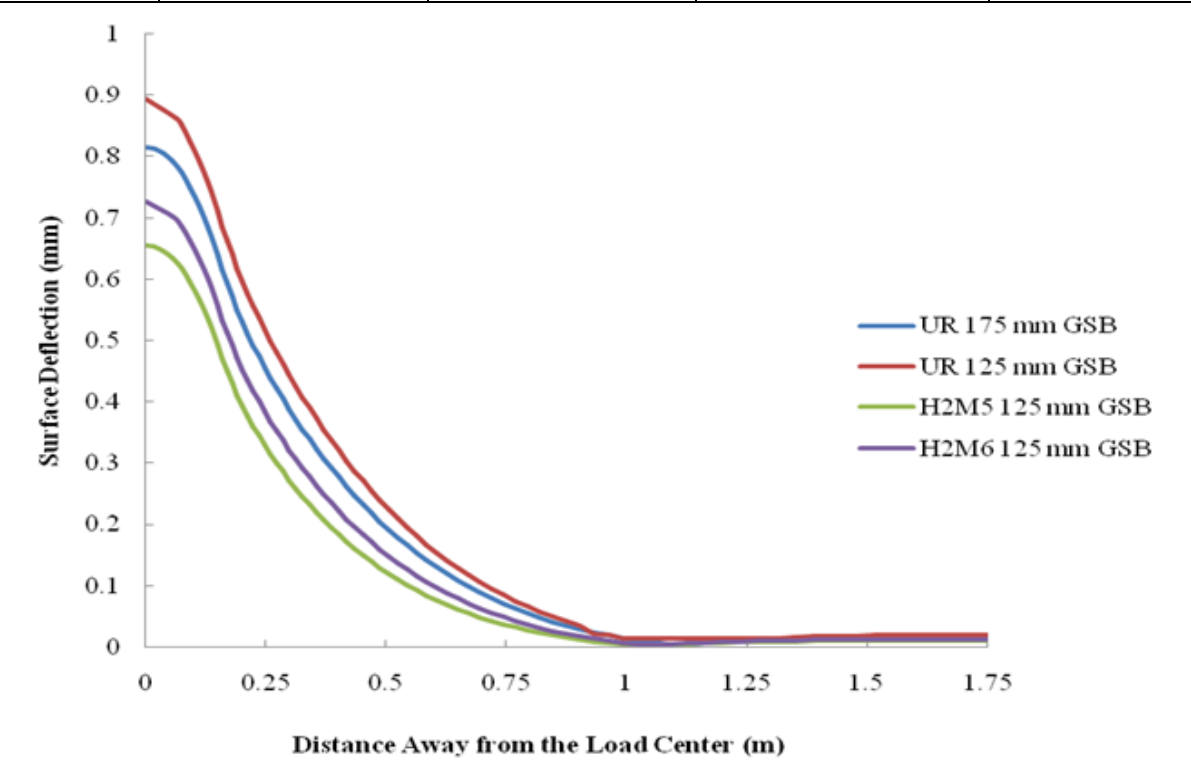


Figure-7: Vertical displacement profile along the width of the pavement section.

Remarkably, the H2M5-reinforced section demonstrated superior subgrade performance despite having a thinner GSB layer than the UR-175 mm section, reinforcing its potential in optimizing pavement thickness. On the other hand, while the H2M6-reinforced section outperformed the unreinforced reduced section, it did not surpass the strain control observed in the thicker unreinforced configuration, suggesting a relatively lower efficiency in mobilizing tensile support.

Strain distribution profiles across the pavement width, as illustrated in Figure-9, revealed that H2M6 reinforcement became more effective at lateral distances exceeding 0.17 m from the load center, where tensile strains were more prominently mobilized. In unreinforced sections, strain

concentrations were distributed more uniformly across the pavement width, indicating less efficient load diffusion. For the H2M5-reinforced section, no visible strain spot was observed beyond 0.85 m, compared to 0.95 m and 0.98 m in the unreinforced and H2M6-reinforced sections, respectively.

These findings suggest that coir geotextiles, particularly the H2M5 variant, function as mechanically responsive inclusions. They effectively mobilize tensile resistance following deformation and play a significant role in limiting vertical strain. This highlights their suitability as sustainable reinforcement solutions in flexible pavement systems, especially for low-volume roads where subgrade strength is often inadequate and material optimization is essential.

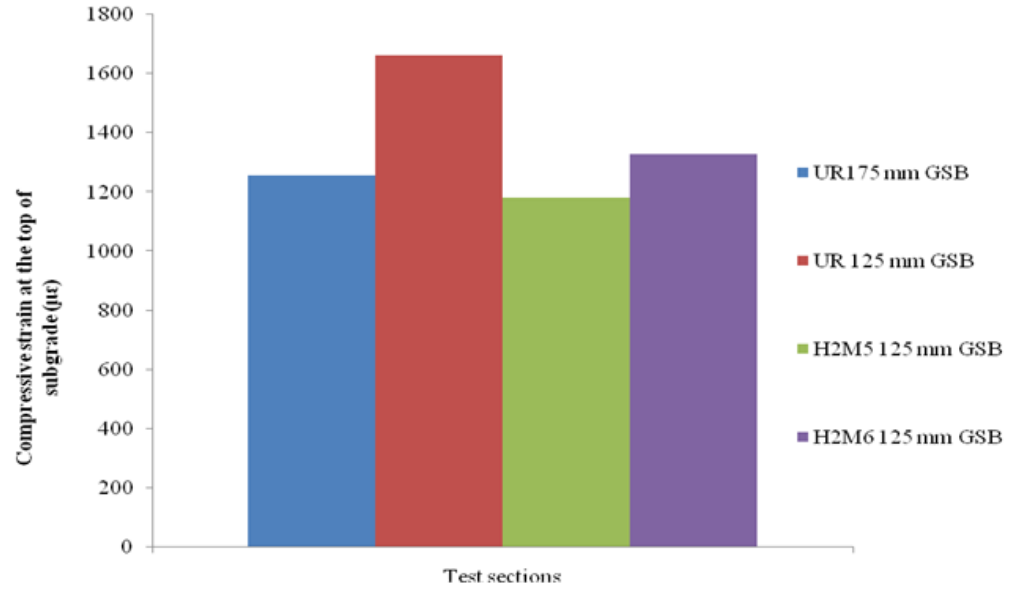


Figure-8: Maximum vertical compressive strain at the top of subgrade layer.

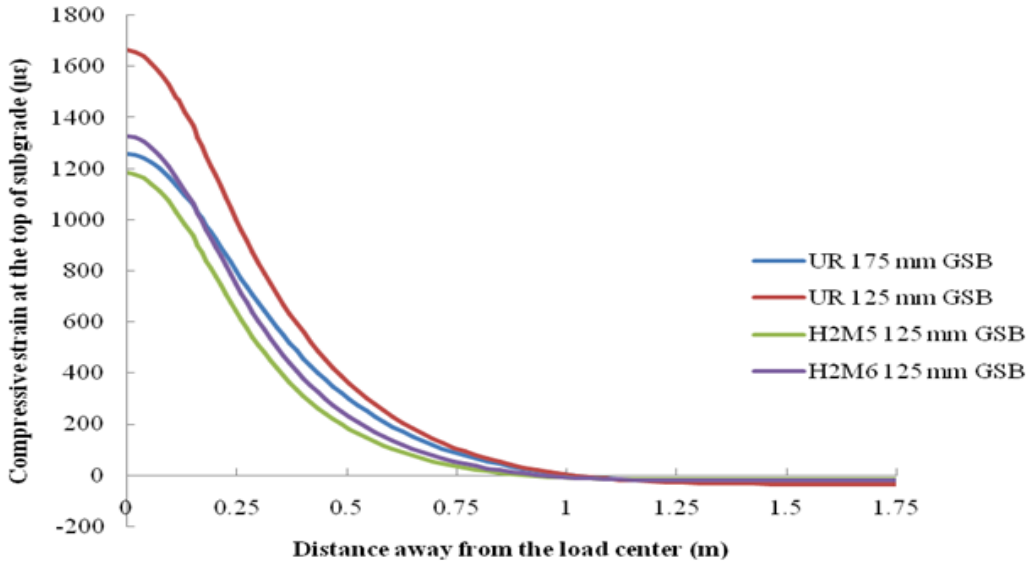


Figure-9: Vertical compressive strain profile along the width of the pavement sections.

Vol. 14(3), 23-33, September (2025)

Conclusion

This study focused on assessing the structural behavior of flexible pavement systems through the incorporation of natural coir geotextiles, specifically H2M5 and H2M6, positioned at the interface between the subgrade and sub-base layers. The evaluation involved conducting laboratory-scale plate load tests to determine and compare the elastic modulus of both reinforced and unreinforced configurations. The experimentally obtained moduli were subsequently used as input parameters for finite element analysis (FEA) using ABAQUS. The numerical investigation considered three pavement configurations with varying granular sub-base (GSB) thicknesses to assess the effectiveness of geotextile reinforcement under different structural conditions. The results consistently demonstrate that coir geotextile reinforcement leads to significant reductions in surface displacement and vertical strain at the subgrade level. Among the two coir geotextile types tested, H2M5 consistently outperformed H2M6, providing superior load distribution and subgrade confinement.

The experimental and numerical results support the following insights: i. The H2M5-reinforced section exhibited an 18% increase in bearing capacity compared to the unreinforced section, whereas the H2M6-reinforced section showed an improvement of only 8%. ii. Reinforcement with H2M5 led to substantial improvement in bearing capacity across all deformation levels, indicating enhanced load resistance throughout the load range. iii. Finite element analysis revealed that the maximum surface displacement was reduced by 27% in the H2M5-reinforced section and by 18% in the H2M6reinforced section relative to the unreinforced configuration. iv. Incorporation of coir geotextiles significantly reduced the vertical strain at the top of the subgrade, with the H2M5reinforced section exhibiting a 29% reduction and the H2M6reinforced section showing a 20% decrease, demonstrating their effectiveness in controlling subgrade deformation. v. At approximately 1-meter radial distance from the center of the applied wheel load, minimal displacement and strain values were observed in the reinforced sections, suggesting effective lateral load distribution and confinement under static loading conditions.

In conclusion, the study confirms that woven coir geotextiles, particularly of type H2M5, significantly enhance the structural behavior of flexible pavements constructed over weak subgrades. Their use not only improves the bearing capacity and stress distribution characteristics of the pavement system but also offers a sustainable and cost-effective alternative to synthetic geosynthetics in low-volume road applications.

Acknowledgement

The study has been conducted as a part of analyzing the coir geotextile reinforced roads laid under the Prime Minister Gram Sadak Yojana (PMGSY) and Bharat Nirman Programmes of Tamil Nadu. The authors gratefully acknowledge the research funding from Coir Board, Ministry of Micro, Small and Medium Enterprises (MSME), Government of India for the project entitled, "Pavement Performance Studies on Coir Geotextile Reinforced Rural Roads in Tamil Nadu".

References

- **1.** Hobbs, N. B. (1986). Mire morphology and the properties and behaviour of some British and foreign peats. *Quarterly Journal of Engineering Geology*, 19, 7–80.
- Hossain, M. S., & Schmidt, B. N. (2009). Benefits of using geotextile between subgrade soil and base coarse aggregate in low-volume roads in Virginia (Final Report VTRC 10-R1). Virginia Transportation Research Council.
- **3.** Flutcher, S., & Wu, J. T. H. (2013). A state-of-the-art review on geosynthetics in low-volume asphalt roadway pavements. *International Journal of Geotechnical Engineering*, 7(4), 411–419.
- Singh, A. K., & Mittal, S. (2018). Analysis of reinforced unpaved roads by modified structural number method. International Journal of Geosynthetics and Ground Engineering, 4(1). https://doi.org/10.1007/s40891-018-0143-4
- **5.** Ismail, I., & Raymond, G. P. (1995). Geosynthetic reinforcement of granular layered soils. In *Geosynthetics* '95, 1, 317–330). Nashville, TN: IFAI, St. Paul, MN, USA.
- **6.** Kinney, T. C., Abbott, J., & Schuler, J. (1998). Benefits of using geogrids for base reinforcement with regard to rutting. *Transportation Research Record: Journal of the Transportation Research Board*, 1611(1), 86–96.
- 7. Cancelli, A., & Montanelli, F. (1999). In-ground test for geosynthetic reinforced flexible paved roads. In *Proceedings of the Conference Geosynthetics* '99 (pp. 863–878). Boston, MA, USA.
- **8.** Leng, J. (2002). Characteristics and behaviour of geogrid reinforced aggregate under cyclic load (Doctoral dissertation). North Carolina State University, Raleigh, USA.
- **9.** Abu-Farsakh, M. Y., & Chen, Q. (2011). Evaluation of geogrid base reinforcement in flexible pavement using cyclic plate load testing. *International Journal of Pavement Engineering*, 12(3), 275–288.
- **10.** Chauhan, M. S., Mittal, S., & Mohanty, B. (2008). Performance evaluation of silty sand subgrade reinforced with fly ash and fibre. *Geotextiles and Geomembranes*, 26, 429–435.
- 11. Nithin, S., Sayida, M. K., & Evangeline, Y. S. (2012). Experimental investigation on coir reinforced subgrade. In *Proceedings of Indian Geotechnical Conference* (pp. B269). December 13–15, Delhi, India.

Res. J. Engineering Sci.

- **12.** Hufenus, R., Rueegger, R., Banjac, R., Mayor, O., Springman, S. M., &Bronnimann, R. (2006). Full-scale field tests on geosynthetic reinforced unpaved roads on soft subgrade. *Geotextiles and Geomembranes*, 24, 21–37.
- **13.** Kamel, M. A., Chandra, S., & Kumar, P. (2004). Behaviour of subgrade soil reinforced with geogrid. *International Journal of Pavement Engineering*, 5(4), 201–209.
- **14.** Wathugala, G. W., Huang, B., & Pal, S. (1997). Numerical simulation of geosynthetic-reinforced flexible pavements. *Transportation Research Record*, 1534, 58–65.
- **15.** Perkins, S. W., &Edens, M. Q. (2002). Finite element and distress models for geosynthetic-reinforced pavements. *International Journal of Pavement Engineering*, 3(4), 239–250.
- **16.** Nazzal, M. D., Abu-Farsakh, M. Y., & Mohammad, L. N. (2010). Implementation of a critical state two-surface model to evaluate the response of geosynthetics reinforced

- pavements. *International Journal of Geomechanics*, 10(5), 202–212.
- **17.** Kim, M., & Lee, J. H. (2013). Effects of geogrid reinforcement in low volume flexible pavement. *Journal of Civil Engineering and Management*, 19(1), 14–32.
- **18.** Abu-Farsakh, M. Y., Gu, J., Voyiadjis, G. J., & Chen, Q. (2014). Mechanistic-empirical analysis of the results of finite element analysis on flexible pavement with geogrid base reinforcement. *International Journal of Pavement Engineering*, 15(9), 786–798.
- 19. IS 15868 (2008). Natural fibre geotextiles.
- **20.** IS 2720-26 (1987). Method of test for soils: determination of pH.
- **21.** 13162-5 (1992). Geotextiles—methods of test, Part 5.